Coupling of infrared radiation to intersubband transitions in multiple quantum wells: The effective-medium approach

M. Załużny and C. Nalewajko
Institute of Physics, M. Curie Skłodowska University, pl. M. Curie Skłodowskiej 1, 20-031 Lublin, Poland
(Received 9 July 1998)

The coupling of infrared radiation to intersubband excitations in multiple-quantum-well structures is discussed theoretically, employing the effective-medium approach. In contrast with previous papers, nonlocal effects in the intersubband optical response of quasi-two-dimensional electrons are taken into account. The transmission and total internal reflection geometries are considered. Special attention is paid to effects induced by (i) multiple reflections in the multiple-quantum-well structure itself, and (ii) the standing-wave effect connected with background phase-matched interferences. The results obtained indicate that the standing-wave effect plays an important role only in the case of thin structures. It can be taken into account by an appropriate modification of Beer's law. Multiple reflections substantially modify the intersubband absorption line shape of structures with a large number of quantum wells and near grazing incidence. A correct description of this modification must take into account even small differences between the dielectric constants of the well and barrier materials. [S0163-1829(99)04020-5]

I. INTRODUCTION

Optical properties of multiple-quantum-well (MQW) structures in the range of intersubband transitions have been studied experimentally and theoretically by many groups (for a review see, e.g., Refs. 1 and 2). In practically all experimental papers, the analysis of infrared (IR) transmittance spectra is performed by application of Beer's law (the traveling-wave approximation). This approximation is equivalent to neglecting effects induced by multiple reflections in a MQW structure itself and in a substrate. In the case of typical Brewster angle geometry, such an approach has a good justification. Because an external angle of incidence in this geometry is close to the Brewster angle, background phase-matched interference effects in the substrate are negligible. Moreover, a small value of the refraction angle ($\approx 17°$ for GaAs) makes the coupling of IR radiation to intersubband transitions weak and consequently effects connected with multiple reflections (electromagnetic coupling) between different quantum wells are also negligible. Many authors (e.g., Refs. 3 and 4) also tried to employ the traveling-wave approximation in the case of total internal reflection (TIR) geometry. Such an approach is very questionable. The role of electromagnetic coupling between quantum wells is then enhanced, since the internal angle of light propagation (φ_{TIR}) is substantially larger than in the case of Brewster geometry. (usually $\varphi_{\mathrm{TIR}} \simeq 45°$, or is even larger).[2,5,6] Moreover, interference between the incident and reflected light at the semiconductor-air or semiconductor-metal interface (the standing-wave effect) substantially modifies the spatial distribution of a normal component of the electric field of IR radiation. (Only this component couples to intersubband transitions.) Experimental results and theoretical estimates reported in Refs. 7 and 8 indicate that the standing-wave effect has a very strong influence on TIR spectra of relatively thin MQW structures. In the above papers absorption spectra were calculated numerically, employing the transfer-matrix method. Each single quantum well (SQW) was treated as a homogeneous slab (with an effective thickness L_{eff}) described by an anisotropic and local dielectric function. [Since the period of the structure is much smaller than the wavelength of the IR radiation, such an approach is practically equivalent to the commonly used local effective-medium approach (LEMA)].[1,9] Unfortunately, a quasi-two-dimensional electron gas (Q2DEG) is strongly inhomogeneous, and its optical response is nonlocal. Consequently, L_{eff} is not a well-defined quantity and, in principle, should be considered as an adjustable parameter. Scalar random-phase-approximation (RPA) calculations show that, only in the case of a system with two parabolic subbands, L_{eff} can be treated as a frequency-independent quantity.[10–13] However, even when a QW has a rectangular shape, the microscopically calculated parameter L_{eff} differs substantially from the QW thickness (L_{QW}). Due to this, the depolarization shift is not described correctly (it is underestimated) by the LEMA if we assume, as in Refs. 7 and 9, that $L_{\mathrm{eff}} = L_{\mathrm{QW}}$. This is a weak point of the LEMA.

A much more sophisticated, fully nonlocal, and retarded approach, (based on the vector RPA and the Green's-function formalism) was recently developed by Liu.[14,15] Numerical results reported in the above papers show that, for a large angle of incidence, electromagnetic coupling between QWs can play an important role in the analysis of IR transmission and TIR spectra of systems with a sufficiently large number of QWs. Unfortunately, the formalism used by Liu is very complex, and requires large numerical calculations. Consequently, it is not amenable to some analytical treatment. Moreover, numerical results reported in the above papers are only qualitatively correct since they were obtained neglecting the diamagnetic current term in the zz component of the nonlocal conductivity tensor. (This term should be incorporated into the paramagnetic term to obtain a correct description of the depolarization effect.[16,17]) Omitting this term leads to a substantial underestimation of the depolariza-

tion shift in highly doped structures. As mentioned, the LEMA also underestimates the depolarization shift. These explain (i) why absorption spectra resulting from the LEMA (with $L_{\rm eff}=L_{\rm QW}$) are practically only slightly redshifted with respect to that obtained by Liu (see Figs. 7 and 8 in Ref. 15), and (ii) why the depolarization shift calculated in the quasi static limit[10] (the scalar RPA) is substantially larger than that reported by Liu (see Fig. 10 in Ref. 15).

The above-mentioned facts have stimulated a modification of the LEMA by taking into account (in the quasi static limit)[10,13] the inhomogeneous character (nonlocal dielectric response) of a Q2DEG. A great advantage of such a ''nonlocal'' effective medium approach (NEMA) is its simplicity and flexibility compared to the approach used by Liu. For example, in contrast with Liu's formalism, we can go beyond the RPA describing an optical response of a Q2DEG. We can also easily take into account the difference between the dielectric constants of the well and barrier materials. (We will show that this type of dielectric mismatch may play a very important role at grazing incidence.)

In Sec. II we discuss the formalism which underlies our computation. The application of the NEMA for systematic studies of IR spectra of MQWs is presented in Sec. III. In this paper, we consider configurations corresponding to the transmission geometry, TIR geometry, and the attenuated total reflection[18] (ATR) geometry. (The waveguide edge-coupling geometry will be discussed in a separate paper.) To our knowledge, no such studies (performed even in the framework of the LEMA) have been published so far. Section IV contains conclusions.

II. THEORETICAL FRAMEWORK

A. Single quantum well

We start this sction with a very brief presentation of the commonly used nonretarded approach to the problem of coupling of a IR radiation to intersubband transitions in a SQW. The quantum-well thickness is much smaller than the wavelength of the IR radiation (λ). The Fermi wave vector is several orders of magnitude larger than a parallel component of the photon wave vector. Thus an external perturbation (incident radiation field) inducing intersubband transitions can be taken in the following form:[10,13]

$$\mathbf{E}^{\rm ext}(t)=\mathbf{E}^{\rm ext}(\omega)\exp(-i\omega t). \tag{1}$$

[For simplicity, here we neglect a small difference between the dielectric constants of the well (ε_w) and barrier (ε_b) materials].

When the radiation is polarized in the x-z plane (the z axis is along the growth direction), the optical absorption per unit area of the SQW can be approximated by[10,19]

$$\begin{aligned}\mathcal{P}_{\rm SQW}(\omega)&=\tfrac{1}{2}\,{\rm Re}\int_{-\infty}^{\infty}\mathbf{j}(z,\omega)\mathbf{E}^{*}(z,\omega)dz\\&=\tfrac{1}{2}\,{\rm Re}\,[\sigma_{xx}^{(2{\rm D})}(\omega)|E_x^{\rm ext}(\omega)|^2+\tilde{\sigma}_{zz}^{(2{\rm D})}(\omega)|E_z^{\rm ext}(\omega)|^2],\end{aligned} \tag{2}$$

where $\mathbf{j}(z,\omega)=[j_x(z,\omega),0,j_z(z,\omega)]$ is the Fourier component of the current density induced in the SQW.

The normal 2D conductivity $\tilde{\sigma}_{zz}^{(2{\rm D})}(\omega)$, defined by

$$\tilde{\sigma}_{zz}^{(2{\rm D})}(\omega)=\frac{1}{E_z^{\rm ext}(\omega)}\int_{-\infty}^{\infty}j_z(z,\omega)dz=\frac{j_z^{(2{\rm D})}(\omega)}{E_z^{\rm ext}(\omega)}, \tag{3}$$

describes the (nonretarded) response of the electron gas to the z component of the external electric field $\mathbf{E}^{\rm ext}$, not the total field $\mathbf{E}$.

The expression for $\tilde{\sigma}_{zz}^{(2{\rm D})}(\omega)$ resulting from the time-dependent local-density approximation, takes the form[10]

$$\tilde{\sigma}_{zz}^{(2{\rm D})}(\omega)=\Lambda\frac{-i}{[\tilde{E}_{21}^2-(\hbar\omega)^2]/2\hbar\omega\Gamma-i}, \tag{4}$$

where $\Lambda=N_S e^2 f_{12}\hbar/2m\Gamma$, $\tilde{E}_{21}\equiv\hbar\tilde{\omega}_{21}$ is the intersubband transition energy modified by the depolarization and exciton like effects, $f_{12}=2m\hbar^{-2}E_{21}z_{21}^2$ is the oscillator strength connected with $1\rightarrow2$ transitions ($f_{12}\approx1$), $\tau=\hbar/\Gamma$ is the dephasing time connected with $1\rightarrow2$ transitions, N_S is the surface electron concentration, and finally, e and m are the charge and effective mass of the electron, respectively. [In this paper we restrict ourselves to the two-parabolic-subband model (with the intersubband spacing $E_{21}\equiv\hbar\omega_{21}$), assuming that only the ground subband is occupied. Bound-free transitions are considered in Ref. 12].

The parallel conductivity appearing in Eq. (2) is defined by

$$\sigma_{xx}^{(2{\rm D})}(\omega)=\frac{1}{E_x^{\rm ext}(\omega)}\int_{-\infty}^{\infty}j_x(z,\omega)dz=\frac{j_x^{(2{\rm D})}(\omega)}{E_x^{\rm ext}(\omega)}. \tag{5}$$

In further discussion, we assume that it has a Drude-like form

$$\sigma_{xx}^{(2{\rm D})}(\omega)=\frac{N_S e^2}{m(\tau_{\|}^{-1}-i\omega)}, \tag{6}$$

where $\tau_{\|}(>\tau)$ is the intrasubband relaxation time. (In numerical calculations we take $\tau_{\|}=\tau$.)

From Eq. (2) we find that the absorptance (equal to the fraction of the incident energy absorbed) of the SQW surrounded by semi-infinite barriers is given by

$$\begin{aligned}A_{\rm SQW}(\omega,\varphi)&=A_{\rm SQW}^{\perp}(\omega,\varphi)+A_{\rm SQW}^{\|}(\omega,\varphi)\\&=A_{\rm SQW}^{\perp}(\omega)\tan(\varphi)\sin(\varphi)+A_{\rm SQW}^{\|}(\omega)\cos(\varphi),\end{aligned} \tag{7}$$

where $A_{\rm SQW}^{\perp(\|)}(\omega)={\rm Re}\,\Lambda_{\perp(\|)}(\omega)$, $\Lambda_{\perp}(\omega)=(4\pi/c\sqrt{\varepsilon_w})\tilde{\sigma}_{zz}^{(2{\rm D})}(\omega)$, $\Lambda_{\|}(\omega)=(4\pi/c\sqrt{\varepsilon_w})\sigma_{xx}^{(2{\rm D})}(\omega)$ and φ is the angle between the z direction and the direction of incidence of the radiation.

In the two-subband limit we have

$$\Lambda_{\perp}(\omega)=\overline{A}\frac{-i}{[\tilde{E}_{21}^2-(\hbar\omega)^2]/2\hbar\omega\Gamma-i}, \tag{8}$$

where $\overline{A}=4\pi\Lambda/c\sqrt{\varepsilon_w}$. Since usually $\Gamma\ll\tilde{E}_{21}$, the frequency dependence of $A_{\rm SQW}^{\perp}(\omega)$ takes practically the Lorentzian shape ($A_{\rm SQW}^{\perp}(\omega)\cong\overline{A}/\{[(\tilde{E}_{21}-\hbar\omega)/\Gamma]^2+1\}$) with the width $=2\Gamma$.

Taking typical for GaAs values of $m=0.066m_0$ and $\varepsilon_w=10.9$, we find that $\overline{A}_{|\mathrm{GaAs}}\simeq 0.016\times f_{12}N_S[10^{11}\mathrm{cm}^{-2}]/\Gamma[\mathrm{meV}]$. Taking $\tilde{E}_{21}/2\Gamma\approx 10$, for estimations, one finds that

$$A^{\perp}_{\mathrm{SQW}}(\tilde{\omega}_{21})/A^{\parallel}_{\mathrm{SQW}}(\tilde{\omega}_{21})\approx\tau\tau_{\parallel}\tilde{\omega}^2_{21}f_{12}/2\sim 200. \tag{9}$$

Thus, except for the case of nearly normal incidence, the relative contribution of intrasubband transitions to $A_{\mathrm{SQW}}(\omega,\varphi)$ is vanishingly small.

In the approach presented above, the reflection of the light by the Q2DEG is completely neglected. It can be easily included employing a more sophisticated approach based on the 2D sheet-model.[19,17] In this model the Q2DEG is treated as a conducting sheet (located at the center of the QW) carrying a sheet current $\mathbf{j}^{(2\mathrm{D})}=(j_x^{(2\mathrm{D})},0,j_z^{(2\mathrm{D})})$. Let us assume that the light is incident at an angle φ (from the left side) on the sheet located (at $z=0$) between semi-infinite identical media with dielectric constant ε_w. Using the jump boundary conditions[19]

$$\begin{aligned}E_x(0^+)-E_x(0^-)&=\frac{4\pi k_x}{\omega\varepsilon_w}j_z^{(2\mathrm{D})}(\omega)\\&=\frac{4\pi k_x}{\omega\varepsilon_w}\tilde{\sigma}_{zz}^{(2\mathrm{D})}(\omega)\frac{D_z(z=0^-,\omega)}{\varepsilon_w},\end{aligned} \tag{10}$$

$$\begin{aligned}H_y(0^+)-H_y(0^-)&=\frac{-4\pi}{c}j_x^{(2\mathrm{D})}(\omega)\\&=\frac{-4\pi}{c}\sigma_{xx}^{(2\mathrm{D})}(\omega)E_x(z=0^-,\omega),\end{aligned} \tag{11}$$

we find that [in the limit $|\Lambda_{\parallel}(\omega,\varphi)\Lambda_{\perp}(\omega,\varphi)|\ll 1$] the reflection ($r^{(2\mathrm{D})}$) and transmission ($t^{(2\mathrm{D})}$) coefficients of the sheet are given by[25]

$$r^{(2\mathrm{D})}=\frac{\Lambda_-(\omega,\varphi)}{1+\Lambda_+(\omega,\varphi)}, \tag{12}$$

$$t^{(2\mathrm{D})}=\frac{1}{1+\Lambda_+(\omega,\varphi)}, \tag{13}$$

where $\Lambda_{\pm}(\omega,\varphi)=\frac{1}{2}[\Lambda_{\parallel}(\omega,\varphi)\pm\Lambda_{\perp}(\omega,\varphi)]$, $\Lambda_{\parallel}(\omega,\varphi)=\Lambda_{\parallel}(\omega)\cos(\varphi)$ and $\Lambda_{\perp}(\omega,\varphi)=\Lambda_{\perp}(\omega)\tan(\varphi)\sin(\varphi)$. If we neglect the Drude-like absorption ($\Lambda_{\parallel}(\omega)=0$) then Eqs. (12) and (13) coincide with that derived in our previous paper.[17]

Since usually $|\Lambda_{\pm}(\omega,\varphi)|\ll 1$ the expression for SQW absorptance resulting from the sheet model ($=1-|r^{(2\mathrm{D})}|^2-|t^{(2\mathrm{D})}|^2$) reduces practically to that given by Eq. (7). The reflectance of the sheet ($=|r^{(2\mathrm{D})}|^2$) is then negligibly small ($\simeq|\Lambda_-(\omega,\varphi)|^2$).

B. Effective-medium approach

Let us consider a nontunneling MQW structure with a period (L_{MQW}) much smaller than λ. (Weakly tunneling structures were discussed in Ref. 20.) Inside the structure Fourier components of the total electric field ($\mathbf{E}$), the generalized displacement ($\mathbf{D}$) and the electron current density induced in the structure ($\mathbf{j}$) are connected by relation[21]

$$\mathbf{D}(z,k_x;\omega)=\varepsilon(z)\mathbf{E}(z,k_x;\omega)+\frac{i4\pi}{\omega}\mathbf{j}(z,k_x;\omega), \tag{14}$$

where $\varepsilon(z)$ is the background dielectric constant at point z, i.e., $\varepsilon(z)=\varepsilon_b(\varepsilon_w)$ in the region occupied by the barrier (well) material, and k_x is a parallel component of the photon wave vector. (The incident radiation is polarized in the x-z plane.)

[Since we work in the long-wavelength limit (LWL) in further discussion, we assume that $\mathbf{j}(z,k_x;\omega)=\mathbf{j}(z,k_x=0;\omega)$. Moreover, in most cases we leave out the reference to k_x in our notation; i.e., we write $\mathbf{D}(z,k_x;\omega)=\mathbf{D}(z,\omega)$, etc.]

Standard boundary conditions require that E_x and D_z are continuous at the interfaces. Since $L_{\mathrm{MQW}}\ll\lambda$ and $A_{\mathrm{SQW}}(\omega,\varphi)\ll 1$, these field components are practically unchanged over the superlattice period. On the other hand, E_z and D_x are not continuous. Thus these quantities may be spatially averaged over the period of the structure

$$\langle D_x(\omega)\rangle=\frac{1}{L_{\mathrm{MQW}}}\int_{-L_{\mathrm{MQW}}/2}^{L_{\mathrm{MQW}}/2}D_x(z',\omega)dz', \tag{15}$$

$$\langle E_z(\omega)\rangle=\frac{1}{L_{\mathrm{MQW}}}\int_{-L_{\mathrm{MQW}}/2}^{L_{\mathrm{MQW}}/2}E_z(z',\omega)dz'. \tag{16}$$

(Writing these equations, we have assumed that the QW occupies the region $|z'|<L_{\mathrm{QW}}/2$.)

The quantities $\langle D_x(\omega)\rangle$ and $\langle E_z(\omega)\rangle$ can be used for definition of the effective dielectric functions[22]

$$\varepsilon_{xx}(\omega)=\langle D_x(\omega)\rangle/E_x(\omega), \tag{17}$$

$$\varepsilon_{zz}^{-1}(\omega)=\langle E_z(\omega)\rangle/D_z(\omega). \tag{18}$$

Employing Eqs. (14)–(16), we find that

$$\langle D_x(\omega)\rangle=\epsilon_{xx}E_x(\omega)+\frac{i4\pi}{\omega L_{\mathrm{MQW}}}\int_{-L_{\mathrm{MQW}}/2}^{L_{\mathrm{MQW}}/2}j_x(z',\omega)dz', \tag{19}$$

$$\langle E_z(\omega)\rangle=\frac{D_z(\omega)}{\epsilon_{zz}}-\frac{i4\pi}{\omega L_{\mathrm{MQW}}\varepsilon_w}\times\int_{-L_{\mathrm{MQW}}/2}^{L_{\mathrm{MQW}}/2}j_z(z',\omega)\frac{\varepsilon_w}{\varepsilon(z')}dz', \tag{20}$$

where $\epsilon_{xx}=(1-f)\varepsilon_b+f\varepsilon_w$, $\epsilon_{zz}^{-1}=(1-f)/\varepsilon_b+f/\varepsilon_w$ and $f=L_{\mathrm{QW}}/L_{\mathrm{MQW}}$.

Since, in the structures considered here, $(\varepsilon_w-\varepsilon_b)\ll\varepsilon_w$, and the ground state wave function is localized mainly in the quantum-well material, the z-dependent dielectric function, appearing in Eq. (20), can be replaced by ε_w. In this approximation electronic contributions to $\langle D_x(\omega)\rangle$, and $\langle E_z(\omega)\rangle$ are determined only by the surface current density $j_x^{(2\mathrm{D})}(\omega)$ and $j_z^{(2\mathrm{D})}(\omega)$, respectively. In further calculations we neglect the influence of retardation effects on $j_z^{(2\mathrm{D})}(\omega)$ and $j_x^{(2\mathrm{D})}(\omega)$ i.e., we assume that the above components of surface current density can be approximated by Eqs. (3) and (5), respectively. [It should be emphasized that the nonretarded limit is employed only to calculate the surface current density; the formulas for reflectance and transmittance of

multilayer structures (with MQWs) derived in this paper retain the retardation.] The approximation used here leads to the following expressions for the principal components of the effective medium dielectric tensor $\boldsymbol{\varepsilon}(\omega)$:

$$\varepsilon_{jj}(\omega)=\epsilon_{xx}+\Delta\varepsilon_{xx}(\omega) \quad j=x,y, \tag{21}$$

$$\frac{1}{\varepsilon_{zz}(\omega)}=\frac{1}{\epsilon_{zz}}-\frac{\Delta\varepsilon_{zz}(\omega)}{\varepsilon_w^2}, \tag{22}$$

where $\Delta\varepsilon_{xx}(\omega)=i4\pi\sigma_{xx}^{(2D)}(\omega)/\omega L_{\mathrm{MQW}}$ and $\Delta\varepsilon_{zz}(\omega)=i4\pi\tilde{\sigma}_{zz}^{(2D)}(\omega)/\omega L_{\mathrm{MQW}}$.

Using Eqs. (4) and (6), we find that

$$\Delta\varepsilon_{xx}(\omega)=\mathcal{L}_{\parallel}(\omega)\frac{-1}{i(\omega\tau_{\parallel})^{-1}+1}, \tag{23}$$

where $\mathcal{L}_{\parallel}(\omega)=4\pi e^2N_S/\omega^2mL_{\mathrm{MQW}}$ and

$$\Delta\varepsilon_{zz}(\omega)=\mathcal{L}_{\perp}(\omega)\frac{1}{[\tilde{E}_{21}^2-(\hbar\omega)^2]/2\hbar\omega\Gamma-i}, \tag{24}$$

with $\mathcal{L}_{\perp}(\omega)=2\pi e^2N_Sf_{12}\hbar/\omega m\Gamma L_{\mathrm{MQW}}$.

In the case of typical GaAs/$Ga_{1-x}Al_xAs$ MQW structures,

$$\mathcal{L}_{\parallel}(\omega)_{|\mathrm{GaAs}}\cong 2.07\times\frac{N_S[10^{12}\ \mathrm{cm}^{-2}]}{L_{\mathrm{MQW}}[100\ \text{Å}]\{\hbar\omega[100\ \mathrm{meV}]\}^2} \tag{25}$$

and

$$\mathcal{L}_{\perp}(\omega)_{|\mathrm{GaAs}}\cong 10.45\times\frac{f_{12}N_S[10^{12}\ \mathrm{cm}^{-2}]}{L_{\mathrm{MQW}}[100\ \text{Å}]\Gamma[10\ \mathrm{meV}]\hbar\omega[100\ \mathrm{meV}]}. \tag{26}$$

The numerical calculations reported in this paper have been performed taking the parameters appropriate for MQW structures studied experimentally (theoretically) in Ref. 5 (Ref. 23), i.e., $\tilde{E}_{21}=111$ meV, $2\Gamma=11.2$ meV, $f_{12}=0.85$, $N_S=1.2\times10^{12}$ cm^{-2}, $\varepsilon_w=10.9$, $L_{\mathrm{MQW}}=405$ Å, $\epsilon_{xx}=10.08$ and $\epsilon_{zz}=10.06$. Only in Fig. 1 do we consider an additional structure with $L_{\mathrm{MQW}}=200$ Å, $\epsilon_{xx}=10.37$, and $\epsilon_{zz}=10.34$. This figure shows the spectral shape of real and imaginary parts of $\varepsilon_{zz}(\omega)$ and $\varepsilon_{xx}(\omega)$ resulting from Eqs. (21) and (22). The presented results indicate that, in the case of typical GaAs/$Ga_{1-x}Al_xAs$ structures, the peak value of $\mathrm{Im}[\varepsilon_{zz}(\omega)]$ is usually smaller than ε_w. It is interesting also to note that the peak value is achieved at the energy (E_{peak}) which is smaller than the SQW resonant energy $\tilde{E}_{21}$. For the structure with $L_{\mathrm{MQW}}=405$ Å(200 Å), the difference ($E_{\mathrm{peak}}-\tilde{E}_{21}$) is rather substantial -2.2 meV (-4.5) meV. Taking $\varepsilon_b=\varepsilon_w$ one finds that $E_{\mathrm{peak}}\cong[\tilde{E}_{21}^2-(\Delta\tilde{E}_{21})^2]^{1/2}$, where $(\Delta\tilde{E}_{21})^2=4\pi N_Se^2\hbar^2f_{12}/m\varepsilon_wL_{\mathrm{MQW}}$. This result is consistent with that reported in Ref. 24.

C. Multilayer optics

The form of dielectric tensor $\boldsymbol{\varepsilon}(\omega)$ indicates that the MQW structure behaves, in the LWL, as a homogenous uniaxial medium. Employing the standard optics equation[1,25]

$$k^2\mathbf{E}-\mathbf{k}(\mathbf{kE})-K^2\boldsymbol{\varepsilon}\mathbf{E}=0, \tag{27}$$

one finds that in such a medium the radiation wave vector is of the form $\mathbf{k}=[k_x,0,k_z^{(\mathrm{MQW})}]$, where

$$(k_z^{(\mathrm{MQW})})^2=\varepsilon_{xx}(\omega)K^2-\frac{\varepsilon_{xx}(\omega)}{\varepsilon_{zz}(\omega)}k_x^2, \tag{28}$$

and $K=\omega/c$ is the wave vector of the radiation in vacuum.

The in-plane component of the wave vector (k_x) must be continuous at an interface. Thus it is the same in an ambient and uniaxial medium and is fixed by the angle of incidence φ (in the ambient medium), $k_x=K\sqrt{\varepsilon_0}\sin(\varphi)$ (ε_0 is the dielectric constant of the ambient medium).

Let us assume for the moment that the MQW structure is infinite, and take $\varepsilon_b=\varepsilon_w$ and $\Delta\varepsilon_{xx}(\omega)=\Gamma=0$. Then one can easily check that the LWL dispersion relation for intersubband plasmon polariton, resulting from Eqs. (28) and (22), coincides with that derived by King-Shmith and Inkson[26] treating the full electrodynamics of the system. This result provides strong evidence to support the NEMA. At this point we would like to emphasize that, contrary to suggestions of some authors,[27] optical properties of finite MQW structures cannot be interpreted in terms of bulk modes of infinite superlattices. The theory developed by Fuchs and Kliewer[28] indicates that not bulk polariton modes but virtual (radiative) modes are responsible for absorption spectra of thin slabs. A more detailed discussion of this problem is beyond the scope of this paper, and will be a subject of a forthcoming paper article.

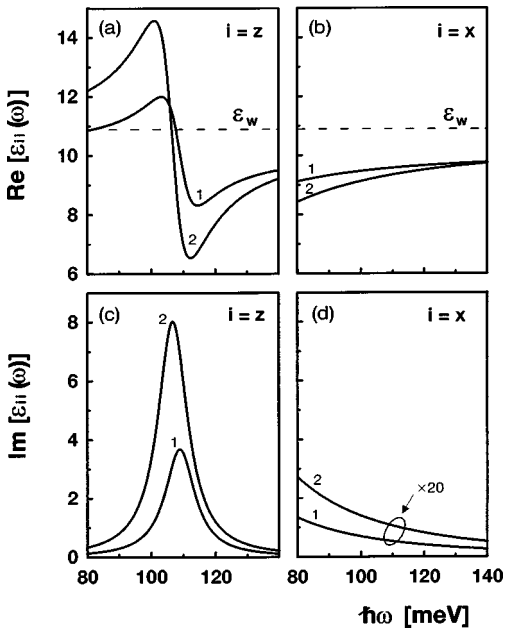

FIG. 1. The spectral characteristics of the real and imaginary parts of $\varepsilon_{zz}(\omega)$ and $\varepsilon_{xx}(\omega)$ for MQW structures with $L_{\mathrm{MQW}}=405$ Å (curves labeled by 1) and $L_{\mathrm{MQW}}=200$ Å (curves labeled by 2).

Modeling reflectance (or transmittance) of typical MQW structures, one discussies a multilayer system. Even if the MQW itself is treated as the effective medium, one must at least account for a substrate and possible buffer or capping layer. Thus we should take into account reflection of the light at different interfaces. The standard transfer-matrix formulation gives an efficient algorithm for an analytical and numerical calculations of the reflection (or transmission) coefficient of multilayer structures. Below, we briefly discuss this method.

Let us consider a multilayer structure that consists of a stack of $1,2,\ldots,m$ plane-parallel layers. Ambient (0) and substrate $(m+1)$ media are semi-infinite. We denote by d_j the thickness of the jth medium ($j\neq 0$, $m+1$). (We assume that only medium $j=j'$, representing the MQW structure, is uniaxial. The thickness of this medium is denoted by $d_{j'} \equiv d_{\mathrm{MQW}}=NL_{\mathrm{MQW}}$ where N is the number of quantum wells in the structure.)

Since incident light is polarized in the x-z plane, the magnetic field is given by $\mathbf{H}(x,z,t)=[0,H_y(z;\omega),0]\exp[i(k_x x-\omega t)]$ i.e., there is a single component of the magnetic field in the y direction. In the jth medium ($j<m+1$) this component can be written in the following form:

$$H_y^{(j)}(z;\omega)=H_{l+}^{(j)}(\omega)\exp[ik_z^{(j)}(z-z_{j,j+1})] + H_{l-}^{(j)}(\omega)\exp[-ik_z^{(j)}(z-z_{j,j+1})], \quad (29)$$

where $z_{j,j+1}=\Sigma_{n=1}^{n=j}d_n$ is the position of $j-j+1$ interface ($j\geqslant 1$) in the z direction, and $z_{0,1}=0$.

For further discussion it is convenient to write the expression for $H_y^{(j)}(z;\omega)(j>0)$ in a slightly modified form:

$$H_y^{(j)}(z;\omega)=H_{u+}^{(j)}(\omega)\exp[ik_z^{(j)}(z-z_{j-1,j})] + H_{u-}^{(j)}(\omega)\exp[-ik_z^{(j)}(z-z_{j-1,j})]. \quad (30)$$

In Eqs. (29) and (30), $H_{\alpha+}^{(j)}(\omega)$ and $H_{\alpha-}^{(j)}(\omega)(\alpha=l,u)$ are complex amplitudes corresponding to waves traveling in positive and negative z directions, respectively. The subscript $l(u)$ indicates that we take the complex amplitude with respect to the plane $z_{j,j+1}(z_{j-1,j})$. From Eq. (28) one finds that the z component of the wave vector appearing in Eqs. (29) and (30) is given by

$$k_z^{(j)}=K\times\begin{cases}\sqrt{\varepsilon_j}\sqrt{1-k_x^2/K^2\varepsilon_j}, & j\neq j'\\ \sqrt{\varepsilon_{xx}}\sqrt{1-k_x^2/K^2\varepsilon_{zz}}, & j=j',\end{cases} \quad (31)$$

where ε_j denotes the dielectric function of the jth medium.

When an angle of incidence is small, the expression for $k_z^{(j')}\equiv k_z^{(\mathrm{MQW})}$ simplifies to the following form:[25]

$$k_z^{(\mathrm{MQW})}=K\sqrt{\varepsilon_w}\cos(\varphi_{\mathrm{int}})\times(1+\kappa), \quad (32)$$

with

$$\kappa=-\frac{\Delta\varepsilon_b}{2\varepsilon_w\cos^2(\varphi_{\mathrm{int}})}+\frac{\Delta\varepsilon_{xx}(\omega)}{2\varepsilon_w}+\frac{\Delta\varepsilon_{zz}(\omega)\tan^2(\varphi_{\mathrm{int}})}{2\varepsilon_w}, \quad (33)$$

where $\Delta\varepsilon_b=\varepsilon_w-\epsilon_{xx}$, $\sin(\varphi_{\mathrm{int}})=\sin(\varphi)\sqrt{\varepsilon_{0w}}$, $\varepsilon_{0w}=\varepsilon_0/\varepsilon_w$ and φ is the angle of incidence in the ambient medium. The above formula is valid as long as $|\kappa|\ll 1$.

Due to the linearity of Maxwell's equations the following relation between amplitudes in the substrate and ambient media may be written:[29,25]

$$\begin{bmatrix}H_{l+}^{(0)}(\omega)\\ H_{l-}^{(0)}(\omega)\end{bmatrix}=\mathbf{T}\begin{bmatrix}H_{u+}^{(m+1)}(\omega)\\ H_{u-}^{(m+1)}(\omega)\end{bmatrix}, \quad (34)$$

where the 2×2 matrix $\mathbf{T}$ is the so-called transfer matrix. It has the following form:

$$\mathbf{T}=\mathbf{I}_{01}\mathbf{L}_1\mathbf{I}_{12}\mathbf{L}_2\ldots\mathbf{L}_m\mathbf{I}_{m(m+1)}. \quad (35)$$

The matrix $\mathbf{L}_j$ describes the effect of propagation through the homogeneous layer j and is given by

$$\mathbf{L}_j=\begin{bmatrix}\exp(-i\beta_j) & 0\\ 0 & \exp(i\beta_j)\end{bmatrix}, \quad (36)$$

where $\beta_j=k_z^{(j)}d_j$.

$\mathbf{I}_{ij}$ is a 2×2 matrix accounting for the interface between the media i and j. Using standard boundary conditions, we find that it can be written in the following form:

$$\mathbf{I}_{ij}=\begin{bmatrix}I_{ij}^{+} & I_{ij}^{-}\\ I_{ij}^{-} & I_{ij}^{+}\end{bmatrix}, \quad (37)$$

with

$$I_{ij}^{\pm}=\frac{k_z^{(i)}\overline{\varepsilon_j}\pm k_z^{(j)}\overline{\varepsilon_i}}{2k_z^{(i)}\overline{\varepsilon_j}}, \quad (38)$$

where $\overline{\varepsilon_j}=\varepsilon_j$ for $j\neq j'$ and $\overline{\varepsilon_{j'}}=\varepsilon_{xx}(\omega)$.

Since in the medium $(m+1)$ there is no backward wave $[H_{u-}^{(m+1)}(\omega)=0]$ the overall transmission (t) and reflection (r) coefficients of the structure are connected with the transfer-matrix components by the relations

$$t=1/T_{11}, \quad r=T_{21}/T_{11}. \quad (39)$$

Having $\mathbf{T}$ [see Eqs. (35)–(38)] we can also derive the components of the electric field in an arbitrary layer employing Maxwell's equation $\nabla\times\mathbf{H}=-i(\omega/c)\mathbf{D}$.

The closed-form expressions for r and t can be obtained only for $m\leqslant 3$. They will be presented in Sec. III.

It is worth discussing an alternative (and more sophisticated) method that can also be applied for description of MQWs. As mentioned, a Q2DEG can be treated as a conducting sheet carrying a sheet current $\mathbf{j}^{(2\mathrm{D})}=(j_x^{(2\mathrm{D})},0,j_z^{(2\mathrm{D})})$. The transfer matrix ($\mathbf{I}^{(2\mathrm{D})}$) accounting for the sheet can be written in the terms of $r^{(2\mathrm{D})}$ and $t^{(2\mathrm{D})}$ defined by Eqs. (12) and (13) (Ref. 25):

$$\mathbf{I}^{(2\mathrm{D})}=\frac{1}{t^{(2\mathrm{D})}}\begin{bmatrix}1 & -r^{(2\mathrm{D})}\\ r^{(2\mathrm{D})} & (t^{(2\mathrm{D})})^2-(r^{(2\mathrm{D})})^2\end{bmatrix}. \quad (40)$$

The transfer matrix of a MQW period ($T^{(\mathrm{per})}$) can be calculated with help of Eqs. (35)–(38). The transfer matrix of a MQW with N wells (T_{MQW}) is connected with $T^{(\mathrm{per})}$ by relation $T_{\mathrm{MQW}}=(T^{(\mathrm{per})})^N$.

Optical spectra presented in Sec. III are obtained employing the NEMA. Nevertheless, we have verified numerically that they coincide with spectra resulting from the sheet

model. This is not a strange result. The polariton dispersion in an infinite superlattices can be derived from the Bloch theorem[30] (see also Ref. 1). This theorem yields $\cos(k_z^{(\mathrm{MQW})}L_{\mathrm{MQW}})=(T_{11}^{(\mathrm{per})}+T_{22}^{(\mathrm{per})})/2$. One can show, performing appropriate Taylor expansions, that the above relation reduces (in the LWL) to the dispersion equation (28) resulting from the NEMA.[25]

III. RESULTS AND DISCUSSION

A. Transmission geometry

At first we discuss a single pass transmission geometry. Let us assume that a MQW structure, approximated by a uniform uniaxial effective layer with a thickness $d_{\mathrm{MQW}}\equiv NL_{\mathrm{MQW}}$ (medium 1), is sandwiched between two transparent semi-infinite overlayer barriers, media 0 and 2, with dielectric constants ε_0 and ε_2, respectively. The radiation (polarized in the x-z plane) incidents from medium 0 at an angle φ.

The transfer-matrix formalism leads to the following expressions for the reflection (r) and transmission (t) coefficients of the system:

$$r=\frac{r_{01}\exp(-i\beta_1)+r_{12}\exp(i\beta_1)}{\exp(-i\beta_1)+r_{01}r_{12}\exp(i\beta_1)}, \tag{41}$$

$$t=\frac{t_{01}t_{12}}{\exp(-i\beta_1)+r_{01}r_{12}\exp(i\beta_1)}, \tag{42}$$

where $\beta_1=k_z^{(\mathrm{MQW})}d_{\mathrm{MQW}}$, and t_{ij} and r_{ij} are the transmission and reflection coefficients for the i-j interface, respectively.

At each interface we have the following relations between t_{ij} and r_{ij}:[29]

$$t_{ij}t_{ji}=1-r_{ij}^2, \tag{43}$$

$$r_{ij}=-r_{ji}. \tag{44}$$

The reflection coefficient appearing in Eqs. (41)–(44) is given by

$$r_{i1}=\frac{k_z^{(i)}\varepsilon_{xx}(\omega)-k_z^{(\mathrm{MQW})}\varepsilon_i}{k_z^{(i)}\varepsilon_{xx}(\omega)+k_z^{(\mathrm{MQW})}\varepsilon_i}=\frac{1-\mathcal{K}_i}{1+\mathcal{K}_i}, \tag{45}$$

with

$$\mathcal{K}_i=\frac{\sqrt{1-\sin^2(\varphi)\varepsilon_0/\varepsilon_{zz}(\omega)}}{\mathcal{N}_i\sqrt{\varepsilon_{xx}(\omega)}}, \tag{46}$$

where $\mathcal{N}_i=\sqrt{\varepsilon_i-\sin^2(\varphi)\varepsilon_0}/\varepsilon_i$, $i=0,2$.

In further discussion we employ the fact that usually $\varepsilon_0=\varepsilon_2=\varepsilon_w$. Then the parameter $\mathcal{K}_0$ (controlling the strength of reflections at 0-1 and 1-2 interfaces) reduces to

$$\mathcal{K}_0=\frac{\sqrt{1-\sin^2(\varphi)\varepsilon_w/\varepsilon_{zz}(\omega)}}{\cos(\varphi)\sqrt{\varepsilon_{xx}(\omega)/\varepsilon_w}}. \tag{47}$$

One can show that when the angle φ is small (more exactly when $|\kappa|\ll 1$) the parameter $\mathcal{K}_0$ is very close to unity. This means that, in the limit $|\kappa|\ll 1$, the reflection amplitude $r_{01}(=-r_{12})$ is vanishingly small.

The reflectance, transmittance and absorptance of the structure are connected with t and r by relations

$$R_{\mathrm{MQW}}(\omega,\varphi)=|r|^2,$$
$$T_{\mathrm{MQW}}(\omega,\varphi)=|t|^2, \tag{48}$$
$$A_{\mathrm{MQW}}(\omega,\varphi)=1-R_{\mathrm{MQW}}(\omega,\varphi)-T_{\mathrm{MQW}}(\omega,\varphi).$$

Simple analytical expressions for $R_{\mathrm{MQW}}(\omega,\varphi)$, $T_{\mathrm{MQW}}(\omega,\varphi)$ and $A_{\mathrm{MQW}}(\omega,\varphi)$ can be obtained in two particular cases: when the structure is thin ($|\beta_1|\ll 1$), or when the angle φ is small. In the case of typical transmission geometry the second condition is practically always fulfilled. Thus the reflection at the 0-1 and 1-2 interfaces can be neglected in the first approximation [$R_{\mathrm{MQW}}(\omega,\varphi)=0$]. Then Eqs. (48) reduce to the commonly used traveling-wave expressions

$$T_{\mathrm{MQW}}(\omega,\varphi)\cong\exp(-2\,\mathrm{Im}\,\beta_1)\cong\exp[-NA_{\mathrm{SQW}}(\omega,\varphi)], \tag{49}$$

$$A_{\mathrm{MQW}}(\omega,\varphi)\cong 1-T_{\mathrm{MQW}}(\omega,\varphi)\cong 1-\exp[-NA_{\mathrm{SQW}}(\omega,\varphi)]. \tag{50}$$

At this point we would like to note that in the case of conventional Brewster angle transmission geometry,[9] we should make the following substitution in Eqs. (49) and (50):

$$A_{\mathrm{SQW}}(\omega,\varphi)\to A_{\mathrm{SQW}}^{\perp}(\omega)\frac{1}{\sqrt{\varepsilon_w(1+\varepsilon_w)}}+A_{\mathrm{SQW}}^{\parallel}(\omega)\sqrt{\frac{\varepsilon_w}{1+\varepsilon_w}}. \tag{51}$$

Numerical calculations show that the above approximation works very well even when structure is very thick ($N\approx 200$).[25] (We have also checked that, near the resonant region, corrections to optical spectra connected with Drude-like contribution are negligible.) The situation is more complex at a grazing incidence. Then the inequality $|\kappa|\ll 1$ is not fulfilled, and the multiple reflections should be taken into account (even when structure is relatively thin).[25] Inspection of Eqs. (41)–(48) suggests that a particularly substantial influence of the electromagnetic coupling on the optical spectra can be expected in the case of thick structures, i.e., when $\overline{\delta}\equiv k_z^{(w)}d_{\mathrm{MQW}}\gg 1[k_z^{(w)}\equiv K\sqrt{\varepsilon_w}\cos(\varphi)]$. The above suggestion is supported by numerical results presented in Fig. 2. Using Eqs. (41)–(48), we have calculated the spectral shapes of $R_{\mathrm{MQW}}(\omega,\varphi)$, $1-T_{\mathrm{MQW}}(\omega,\varphi)$ and $A_{\mathrm{MQW}}(\omega,\varphi)$ for the MQW structure studied experimentally in Ref. 5 at $\varphi=60°$ and 75°. For comparison, the spectral shape of $A_{\mathrm{MQW}}(\omega,\varphi)$ was also calculated employing the traveling-wave equation (50). We find that at a large angle of incidence even a small difference between ε_b and ε_w noticeably modifies MQW optical spectra. This modification is particularly important for $\varphi\geqslant\varphi_c^*$, where $\varphi_c^*=\arcsin\sqrt{\epsilon_{xx}/\varepsilon_w}$ is the critical angle of incidence corresponding to the total internal reflection at the 0-1 interface when $N_S=0$. (In the structure considered here, $\varphi_c^*\simeq 74°$). Unfortunately, experimental verification of our theoretical predictions may be very difficult because work in the range of a large angle of incidence necessitates the use of a special two-prism coupling geometry. Moreover, two quan-

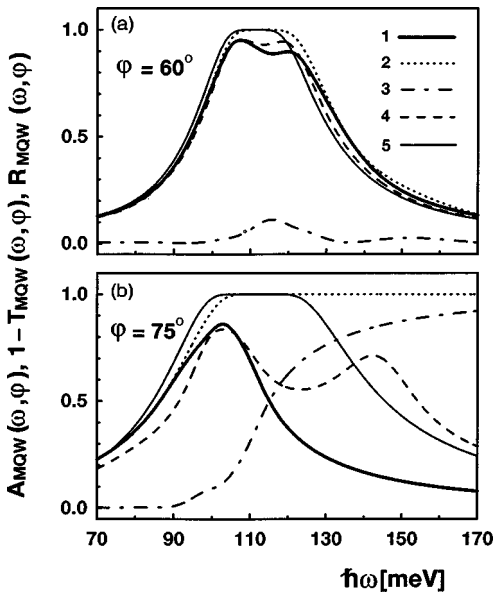

FIG. 2. The spectral dependence of $A_{\mathrm{MQW}}(\omega,\varphi)$ (curves labeled by 1), $1-T_{\mathrm{MQW}}(\omega,\varphi)$ (curves labeled by 2), and $R_{\mathrm{MQW}}(\omega,\varphi)$ (curves labeled by 3) for MQW structures with $N=200$ and $L_{\mathrm{MQW}}=405$ Å, resulting from Eqs. (41), (42), and (48). For comparison we also present the spectral shape of $A_{\mathrm{MQW}}(\omega,\varphi)$, calculated taking $\varepsilon_w=\varepsilon_b$ (curves labeled by 4) and employing the traveling wave approximation (curves labeled by 5). (a) $\varphi=60°$. (b) $\varphi=75°$.

tities $R_{\mathrm{MQW}}(\omega)$ and $T_{\mathrm{MQW}}(\omega)$ have to be measured simultaneously. Such ''drawbacks'' are not inherent in the TIR geometry.

Before we start to discuss the above geometry, we would like to note that, even if we take $\varepsilon_b=\varepsilon_w$, the ω dependence of A_{MQW} predicted by the NEMA only qualitatively coincides with that reported by Liu.[14] As mentioned in Sec. I, this disagreement results from the fact that Liu completely neglected the diamagnetic term in the expression for the zz component of the nonlocal conductivity tensor. One can show (see Ref. 17) that the above approximation is equivalent to the following substitution $N_S\rightarrow(\omega/\omega_{21})^2N_S$ in the expression for $\tilde{\sigma}_{zz}^{(2\mathrm{D})}$. We have verified numerically that this substitution practically removes the difference between the results reported by Liu and that resulting from the NEMA. More detailed discussion of the problem will be given in a separate paper.

B. Total internal reflection geometry

Let us now consider a four-phase system corresponding to the TIR geometry. It is formed by a semi-infinite, medium 0, MQW (medium 1) with a thickness $d_1=d_{\mathrm{MQW}}$, a dielectric medium 2 (cap layer) with thickness d_2, and a semi-infinite medium 3 which can be nearly perfect metal or air. In the latter case we assume that the angle of incidence φ (in medium 0) is larger than the critical angle $\varphi_c^{\mathrm{TIR}}=\arcsin(1/\sqrt{\varepsilon_0})$.

In the absence of a Q2DEG all the incident light will be reflected by the structure. Due to intersubband (and intrasubband) excitations the energy is removed from the incident beam and the reflection coefficient is reduced to less than unity.

The transfer-matrix formalism leads to the following expression for the reflection amplitude of the above multilayer structure:

$$r=\frac{r_{01}\exp(-i\beta_1)+\mathcal{R}_{123}\exp(i\beta_1)}{\exp(-i\beta_1)+r_{01}\mathcal{R}_{123}\exp(i\beta_1)}, \tag{52}$$

with

$$\mathcal{R}_{ijk}=\frac{r_{ij}\exp(-i\beta_j)+r_{jk}\exp(i\beta_j)}{\exp(-i\beta_j)+r_{ij}r_{jk}\exp(i\beta_j)}. \tag{53}$$

The absorptance of the structure is connected with reflectance $R_{\mathrm{MQW}}(\omega,\varphi)=|r|^2$ by the relation

$$A_{\mathrm{MQW}}(\omega,\varphi)=1-R_{\mathrm{MQW}}(\omega,\varphi). \tag{54}$$

As mentioned in Sec. I the TIR spectra are strongly modified by the standing-wave effect. A simplified description of this modification is based on Poynting's theorem. According to this theorem the power absorbed in the effective medium is the power absorbed by unit volume of the layer

$$\mathcal{P}_{\mathrm{MQW}}(z;\omega)=\frac{\omega}{8\pi}\mathrm{Im}\left[\frac{|D_z(z;\omega)|^2}{\epsilon_{zz}^*(\omega)}+\varepsilon_{xx}(\omega)|E_x(z;\omega)|^2\right], \tag{55}$$

integrated over the volume of the layer. Let us assume that the absorption and dispersion of the radiation in the effective medium does not affect a spatial variation of $D_{zz}(z;\omega)$ and $E_x(z;\omega)$ in the structure. Thus they can be calculated taking $\varepsilon_{ii}(\omega)=\varepsilon_w$ and $\varepsilon_0=\varepsilon_2=\varepsilon_w$. The above approximation is well justified when condition $|k_z^{(w)}-k_z^{(\mathrm{MQW})}|d_{\mathrm{MQW}}\simeq|\kappa|\overline{\delta}\ll1$ is fulfilled. Employing Eqs. (55) and (21) we obtain

$$A_{\mathrm{MQW}}(\omega,\varphi)=N[\overline{g_{\mathrm{TIR}}^{\perp}}(\varphi)_{|\omega=\tilde{\omega}_{21}}A_{\mathrm{SQW}}^{\perp}(\omega,\varphi)+\overline{g_{\mathrm{TIR}}^{\parallel}}(\varphi)_{|\omega=\tilde{\omega}_{21}}A_{\mathrm{SQW}}^{\parallel}(\omega,\varphi)], \tag{56}$$

with

$$\overline{g_{\mathrm{TIR}}^{\perp(\parallel)}}(\varphi)=d_{\mathrm{MQW}}^{-1}\int_{d_2}^{d_2+d_{\mathrm{MQW}}}g_{\mathrm{TIR}}^{\perp(\parallel)}(\varphi,z')dz', \tag{57}$$

where $g_{\mathrm{TIR}}^{\perp}(\varphi,z')\equiv|E_z/E_z^{(+)}|^2=2\{1+\cos[2k_z^{(w)}z'+\vartheta_{23}(\varphi)]\}$, $g_{\mathrm{TIR}}^{\parallel}(\varphi,z')\equiv|E_x/E_x^{(+)}|^2=4-g_{\mathrm{TIR}}^{\perp}(\varphi,z')$, and $\mathbf{E}^{(+)}=(E_x^{(+)},0,E_z^{(+)})$ is the electric-field amplitude of the incident light in the medium 0.

Deriving the above expressions we have employed the fact that the reflection coefficient at the 2-3 interface can be written in the form $r_{23}\equiv|r_{23}|\exp[i\vartheta_{23}(\varphi)]$. When medium 3 is a nearly perfect metal ($|\varepsilon_3|\gg1$), then $|r_{23}|\cong1$ and $\vartheta_{23}(\varphi)\cong0$. (We assume that φ is not too close to 90°.) When medium 3 is air and $\varphi\geqslant\varphi_c^{\mathrm{TIR}}$, then $|r_{23}|=1$ and

$$\vartheta_{23}(\varphi)=-2\arctan\{\sqrt{\varepsilon_w[\varepsilon_w\sin^2(\varphi)-1]}/\cos(\varphi)\}. \tag{58}$$

The result equivalent to Eq. (56) was reported by Vodopyanov *et al.*[31] (see also Refs. 32 and 8).

In the limit $d_2, d_{\mathrm{MQW}} \ll 1/k_z^{(w)}$ in Eq. (56) we can make the substitution $\overline{g}_{\mathrm{TIR}}^{\perp(\parallel)}(\varphi) \to g_{\mathrm{TIR}}^{\perp(\parallel)}(\varphi,0)$. When medium 3 is air and $\varphi = 45°$ (which usually takes place) $g_{\mathrm{TIR}}^{\perp}(\varphi,0)$ is much smaller than $g_{\mathrm{TIR}}^{\parallel}(\varphi,0)$. For structures with metal cladding (and φ not too close to 90°) $g_{\mathrm{TIR}}^{\parallel}(\varphi,0) \simeq 0$, $g_{\mathrm{TIR}}^{\perp}(\varphi,0) \simeq 4$, and $A_{\mathrm{MQW}}(\omega,\varphi) \simeq 4NA_{\mathrm{SQW}}^{\perp}(\omega,\varphi)$. The above formula works well only in the limit $4NA_{\mathrm{SQW}}^{\perp}(\omega,\varphi) \ll 1$. When this condition is violated, it overestimates the ''exact'' result substantially.

To obtain the thin layer formula ($\overline{\delta} \ll 1$ and $d_2 = 0$) with a wider range of applications, we employ the approach similar to that used in Ref. 33. Expanding $\exp(\pm i\beta_1)$ to terms of first order in β_1 we find, using Eqs. (45) and (46), that Eq. (41) reduces to

$$r = \frac{(\mathcal{K}_0 - \mathcal{K}_3) + i\beta_1(1 - \mathcal{K}_0\mathcal{K}_3)}{-(\mathcal{K}_0 + \mathcal{K}_3) + i\beta_1(1 + \mathcal{K}_0\mathcal{K}_3)}. \tag{59}$$

It is convenient to rewrite this equation in the following form:

$$r = \frac{\mathcal{N}_0 - \mathcal{N}_3 - i\delta[\sin^2(\varphi)\varepsilon_0/\varepsilon_{zz}(\omega) - 1 + \mathcal{N}_3\mathcal{N}_0\varepsilon_{xx}(\omega)]}{\mathcal{N}_0 + \mathcal{N}_3 + i\delta[\sin^2(\varphi)\varepsilon_0/\varepsilon_{zz}(\omega) - 1 - \mathcal{N}_3\mathcal{N}_0\varepsilon_{xx}(\omega)]}, \tag{60}$$

where $\delta = Kd_{\mathrm{MQW}}$.

When medium 3 is a nearly perfect metal ($|\varepsilon_3| \gg \varepsilon_0$) and φ is not too close to 90° the terms with $\mathcal{N}_3 = \mathcal{N}_3^{\mathrm{metal}} = \sqrt{1 - \sin^2(\varphi)\varepsilon_0/\varepsilon_3}/\sqrt{\varepsilon_3}$ can be omitted. Employing this fact and taking $\varepsilon_0 = \varepsilon_w$, after some manipulations we obtain

$$r = \frac{1 - N\Lambda_{\perp}(\omega,\varphi) + i\overline{\delta}[1 - \tan^2(\varphi)\Delta\varepsilon_b/\varepsilon_b]}{1 + N\Lambda_{\perp}(\omega,\varphi) - i\overline{\delta}[1 - \tan^2(\varphi)\Delta\varepsilon_b/\varepsilon_b]}. \tag{61}$$

Since we work in the thin layer approximation ($\overline{\delta} \ll 1$) the terms containing $\overline{\delta}$ can be neglected. Then the absorptance of the structure is given by

$$A_{\mathrm{MQW}}(\omega,\varphi) = \frac{4N\,\mathrm{Re}\,\Lambda_{\perp}(\omega,\varphi)}{[1 + N\,\mathrm{Re}\,\Lambda_{\perp}(\omega,\varphi)]^2 + [N\,\mathrm{Im}\,\Lambda_{\perp}(\omega,\varphi)]^2}. \tag{62}$$

It is worth noting that, due to the presence of a metal cladding, a parallel component of $A_{\mathrm{SQW}}(\omega,\varphi)$ does not appear in Eqs. (62).

Near resonance [where $\mathrm{Im}\,\Lambda_{\perp}(\omega,\varphi) \ll \mathrm{Re}\,\Lambda_{\perp}(\omega,\varphi)$] we can neglect the term with $\mathrm{Im}\,\Lambda_{\perp}(\omega,\varphi)$. In this limit, $A_{\mathrm{MQW}}(\omega,\varphi)$ can be expressed only by the SQW absorptance $A_{\mathrm{SQW}}^{\perp}(\omega,\varphi) = \mathrm{Re}\,\Lambda_{\perp}(\omega,\varphi)$:

$$A_{\mathrm{MQW}}(\omega,\varphi) = \frac{4NA_{\mathrm{SQW}}^{\perp}(\omega,\varphi)}{[1 + NA_{\mathrm{SQW}}^{\perp}(\omega,\varphi)]^2}. \tag{63}$$

Our numerical calculations show that the above mentioned simplification works very well even far from the resonance if only $NA_{\mathrm{SQW}}^{\perp}(\tilde{\omega}_{21},\varphi) < 1$.

Now we discuss [employing the two parabolic subband expression (8) for $\Lambda_{\perp}(\omega)$] a difference between absorption spectral shape predicted by Eq. (62) and that resulting from Poynting's theorem. Since $\tilde{E}_{21} \ll \Gamma$, near the resonant frequency ($\omega \sim \tilde{\omega}_{21}$) Eq. (62) reduces to the following form:

$$A_{\mathrm{MQW}}(\omega,\varphi) \cong \frac{4\Gamma\Gamma_R}{(\tilde{E}_{21} - \hbar\omega)^2 + (\Gamma + \Gamma_R)^2}, \tag{64}$$

where $\Gamma_R/\Gamma = N\overline{A}\tan(\varphi)\sin(\varphi) = NA_{\mathrm{SQW}}^{\perp}(\tilde{\omega}_{21},\varphi)$.

The absorption spectrum predicted by Eqs. (62) and (64) has, like Poynting's expression, a Lorentzian shape with a peak value at $\omega = \tilde{\omega}_{21}$. However, due to the electromagnetic coupling and attenuation of the IR radiation (which are neglected in Poynting's expression), (i) the linewidth is equal to $2\Gamma \times (1 + \Gamma_R/\Gamma)$ (not 2Γ) and (ii) the peak value is equal to $(4\Gamma_R/\Gamma) \times (1 + \Gamma_R/\Gamma)^{-2}$ (not $4\Gamma_R/\Gamma$). Note that $A_{\mathrm{MQW}}(\tilde{\omega}_{21},\varphi)$ takes the maximum value of 1 when the ratio Γ_R/Γ approaches unity, and then decreases with increasing Γ_R/Γ. Inspection of Eq. (64) also shows that the area under the absorption peak depends explicitly on Γ.

Expressions (61)–(64) are also valid when medium 3 is air ($\varepsilon_3 = 1$) provided that the angle of incidence φ is very close to the critical angle $\varphi_c^{\mathrm{TIR}}[= \arcsin(1/\sqrt{\varepsilon_w})]$. (In this case the factor $\mathcal{N}_3 = \mathcal{N}_3^{\mathrm{air}} = \sqrt{1 - \sin^2(\varphi)\varepsilon_w}$ appearing in Eq. (60) may also be treated as vanishingly small.) When condition $\mathcal{N}_3^{\mathrm{air}} \ll 1$ is not fulfilled a simple expression for $A_{\mathrm{MQW}}(\omega,\varphi)$ can be obtained by substituting Eq. (60) into Eq. (54) and performing an appropriate Taylor expansion. If we retain terms of the first order in $\overline{\delta}$, the resulting expression for the absorptance coincides with that given by Poynting's theorem.

When the MQW structure is very thick ($\overline{\delta} \gg 1$) then $\overline{g}_{\mathrm{TIR}}^{\perp}(\varphi) \approx \overline{g}_{\mathrm{TIR}}^{\parallel}(\varphi) \approx 2$. This suggests that in such structures the standing-wave effect does not affect the reflectance (absorptance) substantially, and the traveling-wave approximation may be used. On the other hand, one can check that for $x < 1$ the function $4x/(1 + x)^2$ is very well approximated by $[1 - \exp(-4x)]$. Thus it is reasonable to assume that, except in the case when the structure is simultaneously very thick and the angle of incidence large, the ''exact'' solution can be simulated by the double pass traveling wave equation with $A_{\mathrm{SQW}}^{\perp(\parallel)}(\omega,\varphi)$ replaced by the effective (averaged) absorptance $\langle A_{\mathrm{SQW}}^{\perp(\parallel)}(\omega,\varphi)\rangle = \frac{1}{2}\overline{g}_{\mathrm{TIR}}^{\perp(\parallel)}(\varphi)_{|\omega=\tilde{\omega}_{21}} A_{\mathrm{SQW}}^{\perp(\parallel)}(\omega,\varphi)$. In this approximation the absorptance of the structure takes the form

$$A_{\mathrm{MQW}}(\omega,\varphi) \simeq 1 - \exp\{-N[\overline{g}_{\mathrm{TIR}}^{\perp}(\varphi)_{|\omega=\tilde{\omega}_{21}} A_{\mathrm{SQW}}^{\perp}(\omega,\varphi) + \overline{g}_{\mathrm{TIR}}^{\parallel}(\varphi)_{|\omega=\tilde{\omega}_{21}} A_{\mathrm{SQW}}^{\parallel}(\omega,\varphi)]\}. \tag{65}$$

Numerical calculations performed in Ref. 25 show that at a typical (for the TIR geometry) angle of incidence $\varphi = 45°$, the above formula works very well at arbitrary thicknesses of the structure. This indicates that the influence of the electromagnetic coupling on absorption spectra is negligibly small when $\varphi \leqslant 45°$. Equation (65) also correctly simulates the ''exact'' result in the range of a large angle of incidence, provided that the MQW structure is very thin ($\overline{\delta} \ll 1$) and $NA_{\mathrm{SQW}}^{\perp}(\tilde{\omega}_{21},\varphi) < 1$. The situation changes drastically when condition $\overline{\delta} \ll 1$ is violated and the angle of incidence is large. In this regime Eq. (65) does not work correctly. This

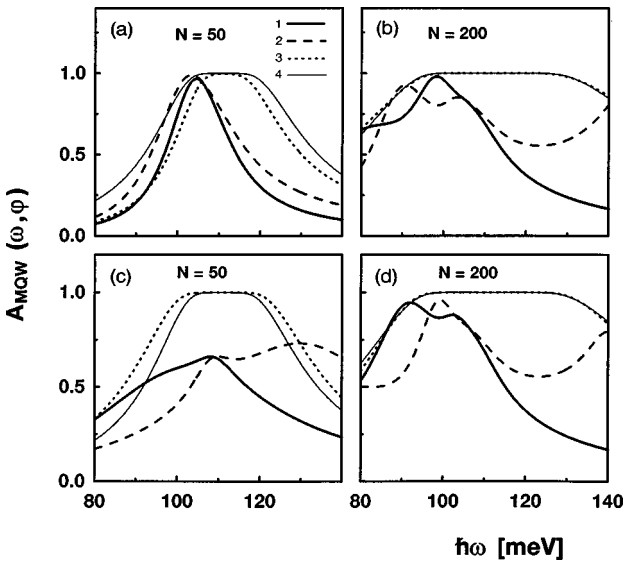

FIG. 3. The spectral dependence of the TIR absorptance of the MQW structures with different numbers of quantum wells: ''exact'' results (curves labeled by 1), ''exact'' results but with $\varepsilon_b=\varepsilon_w$ (curves labeled by 2), results obtained with the help of Eq. (65) (curves labeled by 3), and the traveling wave approximation (curves labeled by 4). (a) and (b) The structure without metal cladding. (c) and (d) The structure with metal cladding. The cap layer thickness $d_2=100$ Å, $\varphi=75°$, and $L_{MQW}=405$ Å.

fact is illustrated in Fig. 3, which presents the TIR absorption characteristics of systems with different numbers of QWs at $\varphi=75°$. Note that, like in the case of the transmission geometry, even a small difference between ε_w and ε_b substantially affects the grazing-incidence absorption line shape.

Figure 4 presents the normalized spatial distribution of $|E_z|^2$ in the structures considered in Fig. 3. (Knowledge of this distribution is, for example, very helpful in a correct interpretation of the resonant second-harmonic generation spectra,[5,23] photon drag effect,[18] or nonlinear intersubband absorption spectra[31].) Inspection of the presented results shows that, in the range of large angle of incidence ($\varphi \geqslant \varphi_c^*$) the standing-wave pattern is destroyed completely, even in the case of relatively thin MQW structures ($N=50$). It is also interesting to note that the spatial distribution of $|E_z|^2$ very strongly depends on a difference between ε_w and ε_b, the frequency of incident light and the presence of metal cladding.

C. Attenuated total reflection geometry

The attenuated total reflection spectroscopy is a well-known method of, for example, chemical analysis to investigate absorption spectra of materials, which are in direct contact with a prism (for a review, see Refs. 34,35). Recently, the above geometry (with a Ge prism) was also used to enhance the coupling of IR radiation with intersubband transitions in $GaAs/Ga_{1-x}Al_xAs$ multiple-quantum-well structures.[18]

Let us consider a multilayer system corresponding to the ATR geometry used in Ref. 18. The system consists of a semi-infinite nonabsorbing medium 0 (prism), a medium 1 (with thickness d_1) which can represent a cap layer (or air gap), a MQW structure (medium 2) with thickness $d_2 \equiv d_{MQW}$, and a semi-infinite dielectric medium 3 with dielectric constant ε_3 smaller than the dielectric constant of the prism ($\varepsilon_0>\varepsilon_3$). We assume that the angle of incidence φ in medium 0 is greater than the critical angle $\varphi_c^{ATR}=\arcsin(\sqrt{\varepsilon_3/\varepsilon_0})$. We also assume for simplicity that $\varepsilon_1=\varepsilon_3=\varepsilon_w$ and take $\varepsilon_0=16$ (then $\varphi_c^{ATR}\simeq 56°$).

As in the case of the TIR geometry, we start from application of Poynting's theorem [see Eq. (55)]. This theorem gives

$$A_{MQW}(\omega,\varphi)=N[\overline{g^{\perp}_{ATR}(\varphi)}_{|\omega=\tilde{\omega}_{21}}A^{\perp}_{SQW}(\omega,\varphi) + \overline{g^{\parallel}_{ATR}(\varphi)}_{|\omega=\tilde{\omega}_{21}}A^{\parallel}_{SQW}(\omega,\varphi)], \quad (66)$$

with

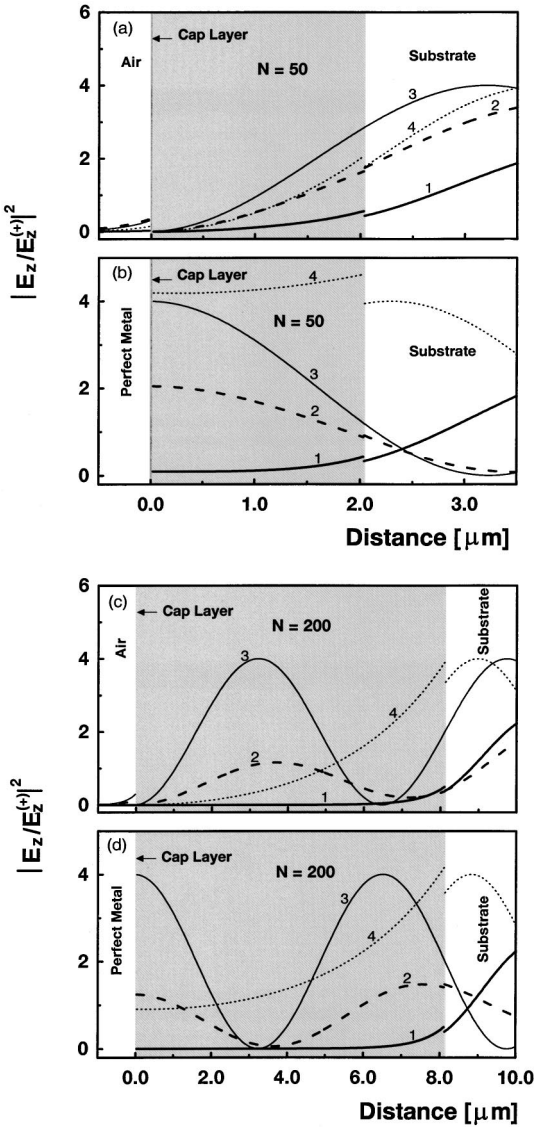

FIG. 4. The spatial variation of $|E_z/E_z^{(+)}|^2$ in the structures considered in Fig. 3 at $\hbar\omega=\tilde{E}_{21}$ (curves labeled by 1) and $\hbar\omega=90$ meV (curves labeled by 2). Curves labeled by 3 (4) show the spatial variation of $|E_z/E_z^{(+)}|^2$ at $\hbar\omega=\tilde{E}_{21}$ calculated taking $\varepsilon_{ii}=\varepsilon_w(\varepsilon_{ii}=\epsilon_{ii})$. The scale of the figure is insufficient to show details of the electric-field variation within the cap layer.

$$\overline{g}^{\perp(\parallel)}_{\mathrm{ATR}}(\varphi)=\frac{g^{\perp(\parallel)}_{\mathrm{ATR}}(\varphi)}{d_{\mathrm{MQW}}}\int_{d_1}^{d_1+d_{\mathrm{MQW}}}\exp(-2|k_z^{(1)}|z)dz, \quad (67)$$

where $g^{\perp}_{\mathrm{ATR}}(\varphi)=2\varepsilon_{0w}^{3/2}\{1+\cos[\vartheta_{01}(\varphi)]\}$, $g^{\parallel}_{\mathrm{ATR}}(\varphi)=2\varepsilon_{0w}^{-1/2}\{1-\cos[\vartheta_{01}(\varphi)]\}$, $|k_z^{(1)}|=K\sqrt{\varepsilon_0\sin^2(\varphi)-\varepsilon_w}$ and $\vartheta_{01}(\varphi)=-2\arctan\{\sqrt{\varepsilon_0}\sqrt{\varepsilon_0\sin(\varphi)^2-\varepsilon_w}/[\varepsilon_w\cos(\varphi)]\}$. [When $d_1, d_{\mathrm{MQW}}\ll 1/|k_z^{(1)}|$, in Eq. (66) we can make the substitution $\overline{g}^{\perp(\parallel)}_{\mathrm{ATR}}(\varphi)\rightarrow g^{\perp(\parallel)}_{\mathrm{ATR}}(\varphi)$. Note that $\overline{g}^{\perp}_{\mathrm{ATR}}(\varphi_c^{\mathrm{ATR}})=g^{\perp}_{\mathrm{ATR}}(\varphi_c^{\mathrm{ATR}})=4\varepsilon_{0w}^{3/2}$.]

Now we derive, starting from Eq. (60) a simplified expression for the absorptance of a thin structure with $d_1=0$. When $\varphi=\varphi_c^{\mathrm{ATR}}$ (or when the difference $\varphi-\varphi_c^{\mathrm{ATR}}$ is very small $\leqslant 0.1°$) the terms containing $\mathcal{N}_3$ can be neglected. Manipulations similar to those used in the case of the TIR geometry show that, the ATR absorptance (at $\varphi\cong\varphi_c^{\mathrm{ATR}}$) can be obtained making in Eqs. (62), (63) and (64) the following substitutions:

$$\varphi\rightarrow\varphi_c^{\mathrm{ATR}}, \quad N\rightarrow N\varepsilon_{0w}^{3/2}. \quad (68)$$

When condition $\varphi\cong\varphi_c^{\mathrm{ATR}}$ is not fulfilled, a simple expression for the reflection amplitude can be obtained performing [in Eq. (60)] an appropriate expansion and neglecting terms higher than the first order in δ. The resulting expression for the absorptance is then identical with that obtained with help of Poynting's theorem.

Analysis of the obtained results suggests that the thin layer ATR absorptance should be well simulated by the following modified traveling-wave equation:

$$A_{\mathrm{MQW}}(\omega,\varphi)\simeq 1-\exp\{-N[\overline{g}^{\perp}_{\mathrm{ATR}}(\varphi)_{|\omega=\tilde{\omega}_{21}}A^{\perp}_{\mathrm{SQW}}(\omega,\varphi)+\overline{g}^{\parallel}_{\mathrm{ATR}}(\varphi)_{|\omega=\tilde{\omega}_{21}}A^{\parallel}_{\mathrm{SQW}}(\omega,\varphi)]\}. \quad (69)$$

Numerical calculations (see Fig. 5 and Ref. 25) support usefulness of the above equation also when $d_1\neq 0$ and $\varphi>\varphi_c^{\mathrm{ATR}}$.

We have calculated (see Fig. 6) the spatial variation of $|E_z|^2$ in the structures considered in Fig. 5. We find that even in the case of thin structures ($N=10$), modification of the above variation (induced by intersubband transitions) can be substantial.

Equation (69) breaks down when the thin layer approximation is violated or/and the cap layer is replaced by an air gap. However, in the last case a substantial simplification of the expression for the absorptance is possible in the limit $\exp(-2|k_z^{(1)}|d_1)\ll 1$ by developing Eq. (39) in a linear approximation of this factor (for details, see Ref. 25).

The situation is much more complex in the case of thick structures. However, when the difference between φ and φ_c^{ATR} is large enough, the condition $\mathrm{Im}\,k_z^{(\mathrm{MQW})}d_{\mathrm{MQW}}\gg 1$ is fulfilled. Then, medium 2 may be treated as semi-infinite. Assuming, additionally, that the cap layer is very thin ($|k_z^{(1)}|d_1\ll 1$), the reflection amplitude of the structure can be approximated by the reflection amplitude corresponding to the prism-effective medium interface (r_{02}) [see Eqs. (37)–(39)] i.e., we can assume that $A_{\mathrm{MQW}}\simeq 1-|r_{02}|^2$. For example, we have checked numerically that for the structure with $N=200$ (50) the above approximation works very well when $\varphi-\varphi_c^{\mathrm{atr}}\geqslant 1°(10°)$.

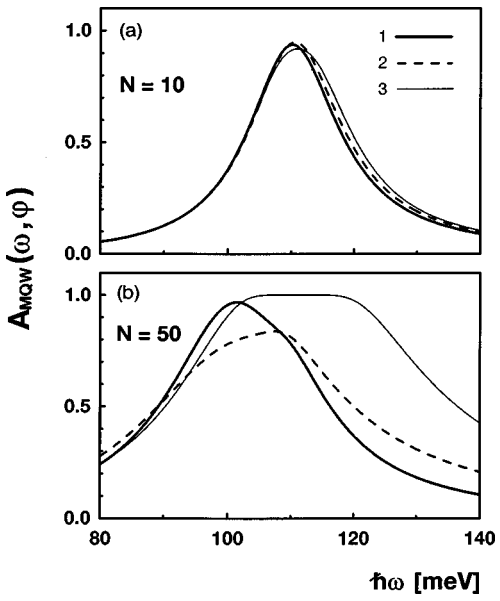

FIG. 5. The spectral dependence of the ATR absorptance of the MQW structures with different numbers of quantum wells at $\varphi=\varphi_c^{\mathrm{ATR}}$: ''exact'' results (curves labeled by 1), ''exact'' results but with $\varepsilon_b=\varepsilon_w$ (curves labeled by 2), and results obtained with the help of Eq. (69) (curves labeled by 3). The cap layer thickness $d_1=100$ Å, $\varepsilon_{|\mathrm{prism}}=16, \varphi_c^{\mathrm{ATR}}\simeq 55.6°$, and $L_{\mathrm{MQW}}=405$ Å.

IV. CONCLUSIONS

In this paper we have modified the commonly used effective-medium approach by including the nonlocal character of intersubband dielectric response of the Q2DEG. The ''nonlocal'' effective-medium approach was then employed for systematic studies of optical properties of MQW structures in the range of intersubband transitions. The obtained

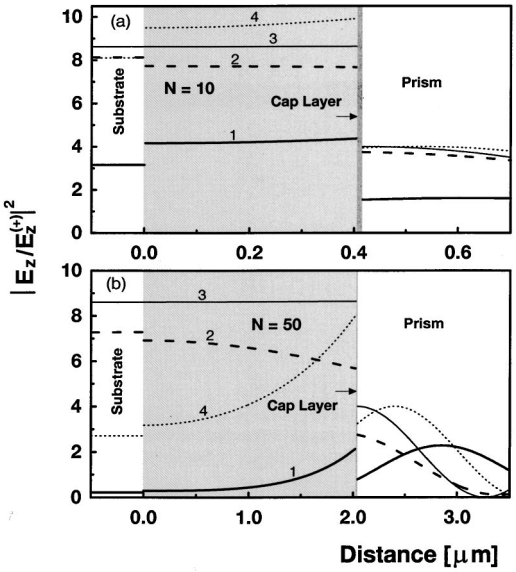

FIG. 6. The spatial variation of $|E_z/E_z^{(+)}|^2$ in the structures considered in Fig. 5 at $\hbar\omega=\tilde{E}_{21}$ (curves labeled by 1) and $\hbar\omega=90$ meV (curves labeled by 2). Curves labeled by 3 (4) show spatial variation of $|E_z/E_z^{(+)}|^2$ at $\hbar\omega=\tilde{E}_{21}$ calculated taking $\varepsilon_{ii}=\varepsilon_w(\varepsilon_{ii}=\epsilon_{ii})$. The scale of the figure is insufficient to show details of the electric-field variation within the cap layer.

results show that, in the case of typical Brewster angle transmission geometry, the absorption spectra can be interpreted employing the traveling-wave approximation. After some modifications the above approximation can also be used for description of TIR spectra (with $\varphi \leqslant 45°$) and thin layer TIR and ATR spectra. However, when the angle of incidence is large and the MQW structure is thick, the modified traveling-wave approximation breaks down completely. The absorption line shape [more exactly $\ln R_{\mathrm{MQW}}^{-1}(\omega)$] deviates then strongly from a Lorentzian shape. A correct description of this deviation must take into account a difference between the dielectric constants of the well and barrier materials.

ACKNOWLEDGMENT

The paper was supported by KBN under Grant No. 2 P03B 072 10.

[1] N. Ray and D. R. Tilley, in *The Dielectric Function of Condensed Systems*, edited by L. V. Keldysh, D. A. Kirzhnitz, and A. A. Maradudin (North-Holland, Amsterdam, 1989).
[2] M. Helm, Semicond. Sci. Technol. **10**, 557 (1995).
[3] B.F. Levine, J. Appl. Phys. **74**, R1 (1993).
[4] G.R.M. de Oliveira, A.M. de Paula, C.L. Cesar, L.C. West, C. Roberts, R.D. Feldman, R.F. Austin, M.N. Islam, and G.E. Marques, Appl. Phys. Lett. **66**, 2382 (1996).
[5] H.C. Liu, J. Li, E. Constard, E. Rosencher, and J. Nagle, Solid-State Electron. **50**, 567 (1996).
[6] A. Seilmeier, H.J. Hübner, G. Abstreiter, G. Weimann, and W. Schlapp, Phys. Rev. Lett. **59**, 1345 (1987).
[7] M.J. Kane, M.T. Emeny, N. Apsley, C.R. Whitehouse, and D. Lee, Semicond. Sci. Technol. **3**, 722 (1988).
[8] J.Y. Andersson and G. Landgren, J. Appl. Phys. **64**, 4123 (1988).
[9] K.B. Ozanyan, O. Hunderi, and B.O. Fimland, J. Appl. Phys. **75**, 5347 (1994).
[10] T. Ando, Z. Phys. B **24**, 219 (1976).
[11] L. Wendler and T. Kraft, Phys. Rev. B **54**, 11 436 (1996).
[12] M. Załużny and C. Nalewajko, J. Appl. Phys. **81**, 3323 (1997).
[13] T. Ando, A. Fowler, and F. Stern, Rev. Mod. Phys. **54**, 437 (1982).
[14] A. Liu, Phys. Rev. B **50**, 8569 (1994).
[15] A. Liu, Phys. Rev. B **55**, 7796 (1997).
[16] D. Dahl and L. Sham, Phys. Rev. B **16**, 651 (1977).
[17] M. Załużny, Physica B **124**, 352 (1984); **128**, 171 (1985).
[18] H. Sigg, S. Graf, M.H. Kwakernaak, B. Margotte, D. Erni, P. van Son, and K. Köhller, Superlattices Microstruct. **19**, 105 (1996).
[19] W.L. Mochan, R. Fuchs, and R.B. Barrera, Phys. Rev. B **27**, 771 (1983).
[20] C. Nalewajko and M. Załużny, Acta Phys. Pol. A **94**, 446 (1998).
[21] L.V. Keldysh, in *The Dielectric Function of Condensed Systems* (Ref. 1).
[22] V. Agranovich and V. Kravtsov, Solid State Commun. **55**, 85 (1985).
[23] E. Rosencher and Ph. Bois, Phys. Rev. B **44**, 11 315 (1991).
[24] T. Ando and S. Mori, J. Phys. Soc. Jpn. **47**, 1518 (1976).
[25] C. Nalewajko, Ph.D. thesis, M. Curie-Skłodowska University, Lublin, 1999 (in Polish).
[26] R.D. King-Smith and J.C. Inkson, Phys. Rev. B **36**, 4796 (1987).
[27] D. Huang, M.O. Manasreh, and G. Gumbs, Phys. Rev. B **54**, 10 980 (1996).
[28] R. Fuchs, K.L. Kliewer, and W.J. Pardee, Phys. Rev. **150**, 589 (1966).
[29] M.A. Azzam and N.M. Bashara, *Ellipsometry and Polarized Light* (North-Holland, Amsterdam, 1987).
[30] L.C. Andreani, Phys. Lett. A **192**, 99 (1994); Phys. Status Solidi B **188**, 29 (1995).
[31] K.L. Vodopyanov, V. Chazapis, C.C. Phillips, B. Sung, and J.S. Harris, Jr., Semicond. Sci. Technol. **12**, 708 (1997).
[32] T. Asano, S. Noda, T. Abe, and A. Sasaki, J. Appl. Phys. **82**, 3385 (1997).
[33] B. Harbeke, B. Heinz, and P. Grosse, Appl. Phys. A: Solids Surf. **38**, 263 (1985).
[34] N.J. Harrick, *Internal Reflection Spectroscopy* (Wiley-Interscience, New York, 1967).
[35] Y.J. Chabal, Surf. Sci. Rep. **8**, 211 (1988).